JOURNAL OF AGRICULTURAL AND FOOD CHEMISTRY

Subscriber access provided by UNIV OF LOUISIANA

New Analytical Methods

Graphene Oxide Quantum Dots Assisted Construction of Fluorescent Aptasensor for Rapid Detection of *Pseudomonas Aeruginosa* in Food Samples

Ran Gao, Zitao Zhong, Xiaomei Gao, and Li Jia

J. Agric. Food Chem., **Just Accepted Manuscript** • DOI: 10.1021/acs.jafc.8b02164 • Publication Date (Web): 24 Sep 2018

Downloaded from http://pubs.acs.org on September 25, 2018

Just Accepted

"Just Accepted" manuscripts have been peer-reviewed and accepted for publication. They are posted online prior to technical editing, formatting for publication and author proofing. The American Chemical Society provides "Just Accepted" as a service to the research community to expedite the dissemination of scientific material as soon as possible after acceptance. "Just Accepted" manuscripts appear in full in PDF format accompanied by an HTML abstract. "Just Accepted" manuscripts have been fully peer reviewed, but should not be considered the official version of record. They are citable by the Digital Object Identifier (DOI®). "Just Accepted" is an optional service offered to authors. Therefore, the "Just Accepted" Web site may not include all articles that will be published in the journal. After a manuscript is technically edited and formatted, it will be removed from the "Just Accepted" Web site and published as an ASAP article. Note that technical editing may introduce minor changes to the manuscript text and/or graphics which could affect content, and all legal disclaimers and ethical guidelines that apply to the journal pertain. ACS cannot be held responsible for errors or consequences arising from the use of information contained in these "Just Accepted" manuscripts.

ACS Publications

is published by the American Chemical Society. 1155 Sixteenth Street N.W., Washington, DC 20036

Published by American Chemical Society. Copyright © American Chemical Society. However, no copyright claim is made to original U.S. Government works, or works produced by employees of any Commonwealth realm Crown government in the course of their duties.

Graphene Oxide Quantum Dots Assisted Construction of Fluorescent Aptasensor for Rapid Detection of *Pseudomonas Aeruginosa* in Food Samples

Ran Gao, Zitao Zhong, Xiaomei Gao, Li Jia*

Ministry of Education Key Laboratory of Laser Life Science & Institute of Laser Life Science, College of Biophotonics, South China Normal University, Guangzhou 510631, China.

*To whom correspondence should be addressed.

Tel: +86-20-85217070

Fax: +86-20-85216052

Email: jiali@scnu.edu.cn

ABSTRACT: We engineered an ingenious fluorescent aptasensor for detection of *Pseudomonas aeruginosa* (*P. aeruginosa*) according to the DNA hybridization and the fluorescence resonance energy transfer. In the absence of target bacteria, 5-carboxyfluorescein-labelled complementary DNA (FAM-cDNA) hybridizes with the partial sequences of aptamer and the fluorescence of FAM can be quenched by graphene oxide quantum dots (GOQDs). Upon the addition of target bacteria, the aptamer as a biorecognition element is bound with *P. aeruginosa* specifically. FAM-cDNA prefers to hybridize with the aptamer, resulting in the desorption of FAM-cDNA from GOQDs, thus recovering the fluorescence of FAM. The aptasensor shows a wide linear response to *P. aeruginosa* in the concentration range of 1.28×10^3 ~ 2.00×10^7 cfu/mL with acceptable selectivity. The detection limit is 100 cfu/mL. The whole process can be finished in 2 hours. Moreover, the platform is successfully applied to detect *P. aeruginosa* in drinking water, orange juice, as well as popsicle samples.

KEYWORDS: *biosensor, bacteria, graphene oxide quantum dots, fluorescent measurement, aptamer, complementary DNA*

INTRODUCTION

Pseudomonas aeruginosa (*P. aeruginosa*), an omnipresent Gram-negative bacterium, is considered as one of the most important causes of nosocomial infections in immunocompromised patients with cancer, transplantation, burn or cystic fibrosis.[1,2] Moreover, *P. aeruginosa* is the main cause of ventilator associated pneumonia.[3] More importantly, *P. aeruginosa* prevalently present in soil, water, as

well as on the surfaces of plants and animals.[4] Thus, environmental water and foods are easy to be contaminated by the bacteria. In order to ensure the food security and protect public health, development of rapid and feasible methods to detect *P. aeruginosa* is extremely important.

The current gold standard method to detect *P. aeruginosa* is culture-based colony counting method. However, the method is inherently time-consuming and labor-intensive since it involves several basic steps (pre-enrichment, selective enrichment and biochemical identification) and usually takes 2-3 days to obtain a confirmed result. In order to overcome these problems of the conventional method, many researchers have geared their efforts towards development of new methods for *P. aeruginosa* detection, such as polymerase chain reaction (PCR)-based method,[5] and enzyme-linked immunosorbent assays (ELISAs).[6] PCR methods involve DNA extraction, PCR amplification, and subsequent gel electrophoresis analysis. These steps usually take several hours and require expertise in molecular biology. ELISAs involve antigen-antibody interactions. Therefore, expensive and labor-intensive biological systems by causing an immune response to the agent are required to produce antibodies. Furthermore, the stability of antibodies is easy to be affected by the sample conditions, such as pH and ionic strength. Thus, development of alternatives to these methods for rapid and selective detection of *P. aeruginosa* is urgently required.

Up to now, significant efforts have been made towards the development of biosensors enabling rapid and selective detection of pathogens.[7-9] Biosensors are now

considered as promising alternatives to the commonly used detection methods for pathogens. A biorecognition element is coupled to a signal transducer to construct a biosensor, in which the transducer is capable of providing a quantitative analytical signal in response to the interaction between the biorecognition element and the target analytes. Among the biorecognition elements, aptamers have increasingly been applied to specifically identify target analytes because they are stable, easily modified, and able to conjugate with target analytes with high affinity and specificity.[10,11] In contrast to antibodies, aptamers demonstrate absolute superiority in the stability and cost. Owing to the unique characteristics of aptamers, they have been adopted as biorecognition elements to construct biosensors (aptasensors) for detection of pathogens, such as *Escherichia coli* (*E. coli*) O157:H7*, Salmonella enterica* (*S. enterica*), and *Staphylococcus aureus* (*S. aureus*).[12,13]

Graphene oxide quantum dots (GOQDs) are nanometer-sized fragments of GO. They are small enough to cause a quantum size effect.[14,15] In recent years, GOQDs have attracted considerable attention because of their fascinating characteristics including strong photoluminescence, chemical inertness, water solubility, excellent biocompatibility, as well as low toxicity.[16,17] In view of these exciting features, GOQDs have been widely explored for fabrication of biosensors, in which, they act as fluorescence reporters for detection of metal ions, glucose, cholesterol, protein, nucleotides, and so on.[18] However, little has been done to exploit the application of GOQDs in the analysis of pathogens. Unlike small molecules and protein macromolecules, pathogens are micro-sized particles. Constructing biosensors to

detect pathogens is more challenging.

GO has been reported to be an efficient energy acceptor in fluorescence resonance energy transfer (FRET). As a result, GO as a good fluorescence quencher is increasingly applied in the fabrication of fluorescent sensors.[19,20] Furthermore, GO can interact with single-stranded DNA nonconvalently by π-π stacking interactions between nucleotide bases and GO.[21,22] In comparison with two-dimensional GO, zero-dimensional GOQDs possess distinct merits such as uniform size distribution, and excellent water solubility. Based on the unique properties of GOQDs, in this study, an ingenious fluorescent aptasensor is designed with the aid of GOQDs for rapid and selective detection of *P. aeruginosa*. In the aptasensor, a label-free aptamer was used as a biorecognition element to identify *P. aeruginosa* specifically, 5-carboxyfluorescein-labelling complementary DNA (FAM-cDNA) was used as a signal reporter to qualify the concentration of *P. aeruginosa*, and GOQDs as an efficient fluorescence quencher. The aptasensor was successfully applied to detect *P. aeruginosa* in drinking water, orange juice, as well as popsicle samples, which demonstrates that the aptasensor has the potential feasibility in real-world samples.

MATERIALS AND METHODS

Reagents and Apparatus. All the reagents were of analytical grade or better. GOQDs (1 mg/mL) were purchased from Nanjing XFNANO Materials Tech Co., Ltd. (Nanjing, China). Sodium chloride (NaCl) and sulfuric acid (H_2SO_4) were purchased from Guangzhou Chemical Reagent Century Technology Company (Guangzhou, China). Potassium chloride (KCl), dipotassium hydrogen phosphate

(K_2HPO_4) and potassium dihydrogen phosphate (KH_2PO_4) were purchased from Guangzhou Chemical Reagent Company (Guangzhou, China). Bovine serum albumin (BSA) was purchased from Shanghai Boao Bio-Science & Technology Company (Shanghai, China). Quinine sulfate dihydrate was purchased from Shanghai Macklin Biochemical Company (Shanghai, China). The oligonucleotides were synthesized by Shanghai Sangon Biological Science & Technology Company (Shanghai, China). Their base sequences are as follows:

P. aeruginosa aptamer:[23] (the complementary base sequences with cDNA are underlined)

5'-CCC CCG TTG CTT TCG CTT TTC CTT TCG CTT TTG TTC GTT TCG TCC CTG CTT CCT TTC TTG-3';

FAM-cDNA (complementary to part of *P. aeruginosa* aptamer):

5'-6-FAM-AC GAA CAA AAG CGA-3'.

The FAM-cDNA and aptamer were dissolved in deionized water and stored at -20 ºC prior to use. Water obtained from an ELGA water purification system (ELGA, London, UK) was used in all experiments.

UV-Vis spectra were recorded on K5600 micro-spectrophotometer (Beijing Kaiao Technology Development Company, Beijing, China). F-380 fluorescence spectrophotometer (Tianjin Gangdong Science & Technology Development Co., Ltd, Tianjin, China) was used to measure fluorescence spectra. Transmission electron microscopy (TEM) images were performed on a JEM-2100HR transmission electron microscope (JEOL, Tokyo, Japan).

Quantum yield measurements. Quinine sulfate was used as the fluorescence standard. The quantum yield of GOQDs (QY_{GOQDs}) was calculated according to the following formula:

$$QY_{\mathrm{GOQDs}} = QY_{\mathrm{st}} \times \frac{I_{\mathrm{GOQDs}}}{I_{\mathrm{st}}} \times \frac{A_{\mathrm{st}}}{A_{\mathrm{GOQDs}}} \times \frac{n_{\mathrm{GOQDs}}^2}{n_{\mathrm{st}}^2}$$

where QY is the quantum yield, I is the integrated emission intensity, A is the absorbance, and n is the refractive index of solvent. The subscript "st" refers to the standard (quinine sulfate).

Preparation of Bacteria Strains. The bacteria strain *P. aeruginosa* (ATCC15442) was cultivated in Luria-Bertani broth (5 mg/mL yeast extract, 10 mg/mL typtone, and 10 mg/mL NaCl, pH 7.0) at 37 ºC for 12 h with shaking at 200 rpm on ZHWY-103B shaker (Shanghai Zhicheng Analytical Instrument Co., Ltd, Shanghai, China). The bacterial cells were collected by centrifugation at 7000 rpm for 3 min and washed twice with phosphate buffer saline (PBS, pH 7.0, 10 mM KH_2PO_4/K_2HPO_4, 137 mM NaCl, 2.7 mM KCl). The concentration of bacteria was adjusted by measuring the optical density at 600 nm (OD_{600}). The bacteria cell numbers were also measured by plate-counting method. Bacterial culturing and sample handing were carried out in a sterile clean room. All the containers were sterilized in an autoclave at 121 ºC for 30 min before and after use.

Fluorescent Detection of *P. aeruginosa*. The GOQDs solution (1 mg/mL, 30 μL) was first added to a 1.5 mL centrifugal tube containing FAM-cDNA (500 nM, 30 μL) in PBS buffer (10 mM, pH 7.0). Next, the mixture was incubated at

37 ºC for 20 min in the dark with shaking at 200 rpm. Then, the GOQDs adsorbing FAM-cDNA (FAM-cDNA@GOQDs) were blocked by 1% BSA in PBS solution (10 mM, pH 7.0). Subsequently, the aptamer of *P. aeruginosa* (500 nM, 30 μL) in PBS solution (10 mM, pH 7.0) was added to the *P. aeruginosa* sample solution (210 μL) and the mixture was incubated at 37 ºC for 30 min with shaking at 200 rpm. Afterwards, the bacteria linked with aptamer (aptamer@bacteria) was added to the tube containing FAM-cDNA@GOQDs with final volume 300 μL and the tube was incubated at 37 ºC for 30 min in the dark with shaking at 200 rpm. Finally, the fluorescence intensity of the mixture was measured with the emission wavelength at 520 nm and excitation wavelength at 494 nm. All experiments were repeated three times.

Real Samples Analysis. The feasibility of the aptasensor was verified by determination of *P. aeruginosa* in drinking water, orange juice, as well as popsicle samples. The samples were all obtained from a local market (Guangzhou, China). The drinking water was used directly. Orange juice samples were diluted 100 times using deionized water since they contain many solid particles. The melted viscous popsicle samples were also diluted 100 times using deionized water before determination. The samples spiked with different concentrations of *P. aeruginosa* were determined.

RESULTS AND DISCUSSION

Characterization of GOQDs. The morphology of GOQDs was characterized by TEM. Figure 1a shows the TEM image of GOQDs. They are

homogeneous with the size distribution in the range of 2-4 nm. Figure 1b shows the UV-vis spectra of GOQDs solution. An absorption peak at about 356 nm is observed, attributed to the n-π* transition of the C=O bond.[24] The fluorescence emission spectra of GOQDs is presented in Figure 1c. They exhibit a maximum emission peak at 465 nm when excited at the optimal wavelength of 380 nm. When aqueous solution of GOQDs is irradiated with UV light at a wavelength of 365 nm, a strong blue fluorescence is observed (inset of Figure 1c). The fluorescence quantum yield is calculated to be 12.4%.

Principle of the Fluorescent Aptasensor for Detection of Bacteria.

The principle of the fluorescent aptasensor for detection of *P. aeruginosa* is shown in Figure 2a. In the aptasensor, a label-free aptamer was used as a biorecognition element to identify *P. aeruginosa* specifically, fluorophore FAM-cDNA was used as a signal reporter to qualify the concentration of *P. aeruginosa*, and GOQDs as an efficient fluorescence quencher. It is worth mentioning that the cDNA was designed to have 14 nucleotides, while the aptamer 60 nucleotides. The bulges and internal loops of free aptamers usually play a pivotal role for the formation of high affinity and specificity target-aptamer complexes through the molecular shape complementarity.[25,26] *P. aeruginosa* aptamer forms a stem-loop with the 5'-portion (G9 to C16) branching off from a larger central loop[23] (Figure S1), which might be the strong binding motif with the target bacteria. The sequence of cDNA was designed to make double helix with the central sequence of aptamer (5'-portion T25 to T38) and the unhybridized flanking region in the aptamer is single-stranded. In the absence

of *P. aeruginosa*, the FAM-cDNA@aptamer complex is adsorbed on the GOQDs surface through the single-stranded flanking region in the aptamer that makes the fluorophore close proximity to GOQDs surface and the fluorescence of FAM-cDNA is quenched by GOQDs owing to the FRET,[27] as shown in Figure 2b. Figure S2 demonstrates that GOQDs have a broad adsorption band due to the existence of sp^2 domains, which effectively overlaps with the emission spectrum of FAM-cDNA. Thus GOQDs can act as an energy acceptor and quench the fluorescence of FAM-cDNA as an energy donor via a FRET process. In contrast, upon the addition of target bacteria, the aptamer as a biorecognition element specifically binds to the bacteria. The FAM-cDNA preferentially hybridizes with the aptamer to form FAM-cDNA@aptamer@bacteria complex, leading to the dissociation of FAM-cDNA from GOQDs, and thus resulting in the restoration of the fluorescence of FAM (Figure 2b). Interestingly, the FAM-cDNA@aptamer complex preferentially binds with bacteria instead of GOQDs. That is to say, the complex demonstrates stronger binding affinity to the target bacteria since the central sequence of aptamer (5'-portion T25 to T38) to make double helix with cDNA is not the strong binding motif. The fluorescent aptasensor has specificity since the aptamer possesses specific recognition ability. The whole detection process can be finished in less than 2 hours. Clearly, the aptasensor can realize the rapid and selective detection of bacteria.

In order to validate the principle of the fluorescent aptasensor for detection of bacteria, several experiments were carried out to prove three speculations. The first speculation is that FAM-cDNA@aptamer complex can be adsorbed by GOQDs. As

shown in Figure 2b, compared to the fluorescence intensity of FAM-cDNA, the decrease of fluorescence intensity of FAM-cDNA@aptamer@GOQDs verifies the adsorption of FAM-cDNA@aptamer complex by GOQDs. Compared to the fluorescence intensity of FAM-cDNA@GOQDs, the slight increase of fluorescence intensity of FAM-cDNA@aptamer@GOQDs indicates that the double helix section in FAM-cDNA@aptamer affects the proximity of the fluorophore FAM to GOQDs, thus leading to the decrease of FRET efficiency. This is because the double helix section in FAM-cDNA@aptamer complex loses the affinity to GOQDs.

The second speculation is that target bacteria and aptamer@bacteria complexes do not bind with GOQDs. Firstly, the GOQDs solution was mixed with *P. aeruginosa*. Then the mixture was incubated and centrifuged at 10000 rpm for 3 min to isolate the bacteria. As shown in Figure S3, the fluorescence intensity of supernatant is about the same as that of GOQDs solution with the emission wavelength at 465 nm and excitation wavelength at 380 nm. The result indicates that the bacteria do not bind with GOQDs. Next, an experiment was carried out to investigate whether the aptamer@bacteria complexes bind with GOQDs. As shown in Figure S4, the fluorescence intensity of supernatant after centrifugation of the mixture (GOQDs+aptamer@bacteria) is about the same as that of GOQDs solution, suggesting that the aptamer@bacteria complex does not bind with GOQDs. Additional experiments were also carried out to prove that centrifugation at 10000 rpm for 3 min does not cause the isolation of GOQDs, but is enough to isolate bacteria from solution. The fluorescence intensity of the GOQDs solution before

centrifugation is about the same as that of supernatant after centrifugation of GOQDs with the emission wavelength at 465 nm and excitation wavelength at 380 nm (Figure S5). Compared to the absorbance of bacteria suspension (10^7 cfu/mL) at 250 nm, the obvious decrease in the absorbance of supernatant after centrifugation indicates that bacteria can be completely isolated from solution through centrifugation at 10000 rpm for 3 min (Figure S6).

The third speculation is that the FAM-cDNA@aptamer complex is not released from the bacteria cell surface. The mixture of FAM-cDNA@GOQDs and aptamer@bacteria was centrifuged at 10000 rpm for 3 min to isolate the FAM-cDNA@aptamer@bacteria complex. Then the fluorescence intensity of supernatant was measured with the emission wavelength at 520 nm and excitation wavelength at 494 nm. As shown in Figure S7, the fluorescence intensity gradually decreases with the increase of the concentration of bacteria. This is due to the decrease of the concentration of FAM-cDNA@aptamer remained in supernatant. Furthermore, the fluorescence intensity of supernatant linearly depends on the logarithm of bacteria concentration ranging from 1.28×10^3 to 2.00×10^7 cfu/mL (Figure S8). The result demonstrates that the FAM-cDNA@aptamer complex is still attached on the surface of bacteria.

Optimization of Assay Conditions. The fluorescence quenching of FAM-cDNA by GOQDs plays a key role for the fabrication of the aptasensor. Thus, the amount of GOQDs was first optimized to ensure the complete adsorption of 50 nM FAM-cDNA by GOQDs. Figure 3 shows that the fluorescence intensity of

FAM-cDNA first dramatically decreases with the increase of the concentration of GOQDs when the concentration of GOQDs is below 0.02 mg/mL. In the concentration range of 0.02 to 0.1 mg/mL, the fluorescence intensity of FAM-cDNA slowly decreases. Beyond 0.1 mg/mL, the decreased fluorescence intensity of FAM-cDNA reaches a plateau, which means that FAM-cDNA is completely adsorbed by GOQDs and no free FAM-cDNA is present in the solution. The quenching efficiency is expressed by $1-F/F_0$, where F is the fluorescence intensity of FAM-cDNA after quenching, and F_0 is the original fluorescence intensity of FAM-cDNA. In this case, the quenching efficiency gradually increases with the increase of concentration of GOQDs and reaches a steady value of 70%. Therefore, 0.1 mg/mL GOQDs was used for subsequent experiments.

Next, the impact of incubation time of FAM-cDNA and GOQDs on the fluorescence quenching process was investigated. The adsorption of FAM-cDNA by GOQDs reaches equilibrium in 20 min, as shown in Figure 4a. In this case, over 70% fluorescence of FAM-cDNA is quenched. Therefore, 20 min was selected as the incubation time of GOQDs and FAM-cDNA. Furthermore, the impact of incubation time of FAM-cDNA@GOQDs and aptamer@bacteria on the restoration of fluorescence was studied. The bacteria are first bound with aptamer to form the aptamer@bacteria complex. As shown in Figure 4b, with the increase of incubation time, the fluorescence intensity increases and reaches a plateau beyond 20 min in the presence of aptamer@bacteria. The result indicates that the FAM-cDNA@aptamer@bacteria complex is formed completely within 20 min. In this

case, the FAM molecules are far away from the surface of GOQDs, leading to the restoration of fluorescence of FAM. Hence, 20 min was selected as the optimal incubation time of FAM-cDNA@GOQDs and aptamer@bacteria.

Analytical Performance for *P. aeruginosa*. The fluorescence emission spectra of GOQDs-based aptasensor upon the addition of increasing concentrations of *P. aeruginosa* and the calibration plot for the bacteria detection are demonstrated in Figure 5. As shown in Figure 5a. the fluorescence intensity of the GOQDs-based aptasensor dramatically increases with the increasing concentration of bacteria from 0 to 2.00×10^7 cfu/mL. The result also confirms that the restoration of fluorescence results from the target bacteria. Conversely, in the absence of bacteria, the central sequence of aptamer hybridizes with the FAM-cDNA and the complex is still adsorbed by GOQDs through the unhybridized single-stranded flanking region in the aptamer that makes FAM close proximity to GOQDs surface. Thus the fluorescence of FAM-cDNA is quenched by GOQDs.

The calibration plot for bacteria detection is shown in Figure 5b. The recovering fluorescence intensity linearly depends on the logarithm of bacteria concentration ranging from 1.28×10^3 to 2.00×10^7 cfu/mL. The fitting equation is $F\text{-}F_0 = 693.3 \log C - 1783$ with a determination coefficient (R^2) of 0.9565, where $F\text{-}F_0$ is the recovering fluorescence intensity and C is the concentration of bacteria. The detection limit (LOD) is estimated to be 100 cfu/mL (LOD = 3SD/slope, in which SD is the standard deviation for the blank solution, n = 20).

Specificity of the Fluorescent Aptasensor. To assess the specificity of

the constructed fluorescent aptasensor for *P. aeruginosa*, the influences of some other pathogens, including *E. coli* O157:H7*, S. aureus* and *S. enterica* were examined. The concentration of each bacterium is 10^5 cfu/mL. As shown in Figure 6, in comparison with the negative controls, a significant fluorescence restoration is induced upon the addition of *P. aeruginos*a. Moreover, the fluorescence enhancement in the presence of target bacteria is more than 7-times than those of negative controls. The result clearly demonstrates that the aptasensor is appropriate for selective detection of *P. aeruginosa.* The specificity of the aptasensor for *P. aeruginosa* is attributed to the special recognition ability of aptamer for its target.

Real Samples Analysis. To demonstrate the feasibility of the constructed fluorescent aptasensor in real samples, drinking water, orange juice, as well as popsicle were used as the model samples. The pre-treated samples spiked with different concentrations of *P. aeruginosa* were analyzed. As shown in Table 1, the recoveries range from 93.9% to 108% with relative standard deviation (RSD) less than 6.0%. The results suggest that the proposed fluorescent aptasensor is suitable for rapid and selective detection of *P. aeruginosa* in food samples.

The fabricated aptasensor was compared with GO-based aptasensor which uses FAM-cDNA or FAM-aptamer. Firstly, GO, aptamer and FAM-cDNA were applied for construction of an aptasensor. As shown in Figure S9, although GO can quench the fluorescence of FAM-cDNA, after addition of aptamer@bacteria complexes, the change of fluorescence intensity does not have a linear response against the logarithm of bacteria concentration. We speculate that the difference in size of GO and GOQDs

might have great effect on the construction of aptasensor. The micrometer-sized GO might affect the release of FAM-cDNA@aptamer complex from its surface. Next, using GO and FAM-aptamer to construct an aptasensor for detection of *P. aeruginosa* was investigated. As shown in Figures S10 and S11, the recovering fluorescence intensity has not a good linear response against the logarithm of bacteria concentration in the range of 1.28×10^3 to 2.00×10^7 cfu/mL. The determination coefficient is 0.7772. GOQDs and GO have similar chemical structures and they both serve as effective quenchers in designing fluorescence aptasensors. However, the significant difference in size affects the response of fluorescence intensity of the constructed aptasensor against the concentration of micrometer-sized bacteria. Using GOQDs as a quencher demonstrates a good linear response against the logarithm of bacteria concentration.

The fabricated aptasensor was also compared with previously reported aptasensors targeting at *P. aeruginosa* detection.[28-31] Table 2 displays that the fabricated fluorescent aptasensor demonstrates superiority in the detection speed and linear range although its LOD is slightly higher than those of some previously reported aptasensors.[28-30] In addition to water sample, the aptasensor can be applied for determination of complex food samples. Interestingly, the aptasensor provides a two-way confirmative assay for determination of *P. aeruginosa*. One is to measure the recovering fluorescence intensity resulted from FAM-cDNA@aptamer@bacteria complex (Figure 5b). Another one is to measure the fluorescence intensity of supernatant after centrifugation of FAM-cDNA@aptamer@bacteria complex (Figure

S8).

In summary, a convenient and ingenious fluorescent aptasensor was fabricated for *P. aeruginosa* detection by integrating aptamer, FAM-cDNA and GOQDs. GOQDs with excellent water solubility exhibit a good fluorescence quenching ability for FAM-cDNA@aptamer complex. Upon the addition of target bacteria, the complex demonstrates higher affinity for target bacteria rather than GOQDs, which plays a crucial role for fabrication of the aptasensor. The special recognition ability of aptamer for its target endows the aptasensor with the specificity for *P. aeruginosa*. Furthermore, the successfully rapid detection of target bacteria in real samples indicates the feasibility of the aptasensor in practical applications.

AUTHOR INFORMATION

Corresponding Author

*Tel.: +86 20 85217070. Fax: +86 20 85216052. E-mail: jiali@scnu.edu.cn.

ORCID

Li Jia: 0000-0002-1979-5128

Funding

This work is financially supported by the National Natural Science Foundation of China (21675056) and the Scientific and Technological Planning Project of Guangzhou City (201805010002).

Notes

The authors declare no competing financial interest.

ABBREVIATIONS USED

FAM-cDNA, 5-carboxyfluorescein-labelled complementary DNA; GOQDs, graphene oxide quantum dots; cDNA, complementary DNA; PCR, polymerase chain reaction; ELISAs, enzyme-linked immunosorbent assays; FRET, fluorescence resonance energy transfer; NaCl, sodium chloride; KCl, potassium chloride; K_2HPO_4, dipotassium hydrogen phosphate; KH_2PO_4, potassium dihydrogen phosphate; BSA, bovine serum albumin; PBS, phosphate buffer saline; LOD, limit of detection; RSD, relative standard deviation; TEM, transmission electron microscopy; QY, quantum yield.

REFERENCES

(1) Hashimoto, M.; Sugawara, Y.; Tamura, S.; Kaneko, J.; Matsui, Y.; Kokudo, N.; Makuuchi, M. *Pseudomonas aeruginosa* infection after living-donor liver transplantation in adults. *Transpl. Infect. Dis.* **2009**, *11*, 11–19.

(2) Weisner, A. M.; Chart, H.; Bush, A.; Davies, J. C.; Pitt, T. L. Detection of antibodies to *Pseudomonas aeruginosa* in serum and oral fluid from patients with cystic fibrosis. *J. Med. Microbiol.* **2007**, *56*, 670–674.

(3) El Solh, A. A.; Akinnusi, M. E.; Wiener-Kronish, J. P.; Lynch, S. V.; Pineda, L. A.; Szarpa, K. Persistent infection with *Pseudomonas aeruginosa* in ventilator-associated pneumonia. *Am. J. Respir. Crit. Care Med.* **2008**, *178*, 513–519.

(4) Cuttelod, M.; Senn, L.; Terletskiy, V.; Nahimana, I.; Petignat, C.; Eggimann, P.; Bille, J.; Prod'hom, G.; Zanetti, G.; Blanc, D. S. Molecular epidemiology of *Pseudomonas aeruginosa* in intensive care units over a 10-year period (1998-2007). *Clin. Microbiol. Infect.* **2011**, *17*, 57–62.

(5) Xu, J.; Moore, J. E.; Murphy, P. G.; Millar, B. C.; Elborn, J. S. Early detection of *Pseudomonas aeruginosa* – comparison of conventional versus molecular (PCR) detection directly from adult patients with cystic fibrosis (CF). *Ann. Clin. Microbiol. Antimicrob.* **2004**, *3*, 1–5.

(6) Kurupati, P.; Kumarasinghe, G.; Laa Poh, C. Direct identification of *Pseudomonas aeruginosa* from blood culture bottles by PCR-enzyme linked immunosorbent assay using *oprI* gene specific primers. *Mol. Cell. Probes* **2005**, *19*, 417–421.

(7) Arora, P.; Sindhu, A.; Dilbaghi, N.; Chaudhury, A. Biosensors as innovative tools for the detection of food borne pathogens. *Biosens. Bioelectron.* **2011**, *28*, 1–12.

(8) Ellairaja, S.; Krithiga, N.; Ponmariappan, S.; Vasantha, V. S. Novel pyrimidine tagged silver nanoparticle based fluorescent immunoassay for the detection of *Pseudomonas aeruginosa*. *J. Agric. Food Chem.* **2017**, *65*, 1802–1812.

(9) Yoo, S. M.; Lee, S. Y. Optical biosensors for the detection of pathogenic microorganisms. *Trends Biotechnol.* **2016**, *34*, 7–25.

(10) Stoltenburg, R.; Reinemann, C.; Strehlitz, B. SELEX–a (r) evolutionary method to generate high-affinity nucleic acid ligands. *Biomol. Eng.* **2007**, *24*, 381–403.

(11) Nimjee, S. M.; Rusconi, C. P.; Sullenger, B. A. Aptamers: an emerging class of therapeutics. *Annu. Rev. Med.* **2005**, *56*, 555–583.

(12) Alizadeh, N.; Memar, M. Y.; Moaddab, S. R.; Kafil, H. S. Aptamer-assisted novel technologies for detecting bacterial pathogens. *Biomed. Pharmacother.* **2017**, *93*, 737–745.

(13) Wu, W.; Fang, Z.; Zhao, S.; Lu, X.; Yu, L.; Mei, T.; Zeng, L. A simple aptamer

biosensor for *Salmonellae enteritidis* based on fluorescence-switch signaling graphene oxide. *RSC Adv.* **2014**, *4*, 22009–22012.

(14) Wei, J.; Qiu, J.; Ren, L.; Zhang, K.; Wang, S.; Weeks, B. Size sorted multicolor fluorescence graphene oxide quantum dots obtained by differential velocity centrifugation. *Sci. Adv. Mater.* **2014**, *6*, 1-8.

(15) Liu, F.; Jang, M. H.; Ha, H. D.; Kim, J. H.; Cho, Y. H.; Seo, T. S. Facile synthetic method for pristine graphene quantum dots and graphene oxide quantum dots: origin of blue and green luminescence. *Adv. Mater.* **2013**, *25*, 3657–3662.

(16) Liu, B.; Xie, J.; Ma, H.; Zhang, X.; Pan, Y.; Lv, J.; Ge, H.; Ren, N.; Su, H.; Xie, X.; Huang L.; Huang W. From graphite to graphene oxide and graphene oxide quantum dots. *Small* **2017**, *13*, 1–7.

(17) Lai, E. Carbon, graphene and graphene oxide quantum dots for analytical biochemistry research. *Biochem. Anal. Biochem.* **2016**, *5*, 1–2.

(18) Xie, R.; Wang, Z.; Zhou, W.; Liu, Y.; Fan, L.; Li, Y.; Li, X. Graphene quantum dots as smart probes for biosensing. *Anal. Methods* **2016**, *8*, 4001–4016.

(19) Duan, N.; Gong, W.; Wang, Z.; Wu, S. An aptasensor based on fluorescence resonance energy transfer for multiplexed pathogenic bacteria determination. *Anal. Methods* **2016**, 8, 1390-1395.

(20) Dong, H.; Gao, W.; Yan, F.; Ji, H.; Ju, H. Fluorescence resonance energy transfer between quantum dots and graphene oxide for sensing biomolecules. *Anal. Chem.* **2010**, 82, 5511–5517.

(21) He, S.; Song, B.; Li, D.; Zhu, C.; Qi, W.; Wen, Y.; Wang, L.; Song, S.; Fang, H.;

Fan, C. A graphene nanoprobe for rapid, sensitive, and multicolor fluorescent DNA analysis. *Adv. Funct. Mater.* **2010**, *20*, 453–459.

(22) Liu, Z.; Su, X. A novel fluorescent DNA sensor for ultrasensitive detection of *Helicobacter pylori*. *Biosens. Bioelectron.* **2017**, *87*, 66–72.

(23) Wang, K. Y.; Zeng, Y. L.; Yang, X. Y.; Li, W. B.; Lan, X. P. Utility of aptamer-fluorescence in situ hybridization for rapid detection of *Pseudomonas aeruginosa*. *Eur. J. Clin. Microbiol. Infect. Dis.* **2011**, *30*, 273–278.

(24) Jang, M.-H.; Ha, H. D.; Seo, T. S.; Cho, Y.-H. Direct comparison of optical properties from graphene oxide quantum dots and graphene oxide. *Appl. Sci. Converg. Technol.* **2015**, *24*, 111–116.

(25) Hermann, T.; Patel, D. J. Adaptive recognition by nucleic acid aptamers. *Science* **2000**, *287*, 820–825.

(26) Patel, D. J.; Suri, A. K.; Jiang, F.; Jiang, L.; Fan, P.; Kumar, R. A.; Nonin, S. Structure, recognition and adaptative binding in RNA aptamer complexes. *J. Mol. Biol.* **1997**, *272*, 645–664.

(27) Zheng, P.; Wu, N. Fluorescence and sensing applications of graphene oxide and graphene quantum dots: A review. *Chem. Asian J.* **2017**, 12, 2343–2353.

(28) Jia, F.; Xu, L.; Yan, W.; Wu, W.; Yu, Q.; Tian, X.; Dai, Rui.; Li, Xing. A magnetic relaxation switch aptasensor for the rapid detection of *Pseudomonas aeruginosa* using superparamagnetic nanoparticles. *Microchim. Acta* **2017**, 184, 1539–1545.

(29) Hu, J.; Fu, K.; Bohn, P. W. Whole-cell *Pseudomonas aeruginosa* localized surface plasmon resonance aptasensor. *Anal. Chem.* **2018**, 90, 2326–2332.

(30) Kim, L. H.; Yu, H. W.; Kim, Y. H.; Kim, I. S.; Jang, A. Potential of fluorophore labeled aptamers for *Pseudomonas aeruginosa* detection in drinking water. *J. Korean Soc. Appl. Biol. Chem.* **2013**, *56*, 165–171.

(31) Peleg, A. Y.; Tilahun, Y.; Fiandaca, M. J.; D'Agata, E. M. C.; Venkataraman, L.; Moellering, R. C.; Eliopoulos, G. M. Utility of peptide nucleic acid fluorescence in situ hybridization for rapid detection of *Acinetobacter* spp. and *Pseudomonas aeruginosa*. *J. Clin. Microbiol.* **2009**, *47*, 830–832.

Table 1. Recovery experiments of *P. aeruginosa* in real samples by the fluorescent aptasensor (n = 9)

samples	spiked concentration (cfu/mL)	measured concentration (cfu/mL)	recovery (%)	RSD (%, n = 3)
water	5.70×10^3	5.73×10^3	101	5.4
	2.82×10^4	3.03×10^4	107	1.6
	1.91×10^5	1.80×10^5	94.2	2.7
juice	6.10×10^3	6.06×10^3	99.3	4.0
	3.30×10^4	3.14×10^4	95.2	3.1
	1.56×10^5	1.68×10^5	108	3.6
popsicle	6.00×10^3	6.34×10^3	106	4.4
	4.10×10^4	3.85×10^4	93.9	1.7
	1.68×10^5	1.71×10^5	102	6.0

Table 2. Comparison of the fabricated fluorescent aptasensor with previously reported aptasensors targeting at *P. aeruginosa* detection

detection method	signal reporter	detection limit (cfu/mL)	linear range (cfu/mL)	detection time (h)	reference
magnetic relaxation switch	aptamer modified magnetic particles	50	$10^2 \sim 10^6$	4.7	28
localized surface plasmon resonance	aptamer-neutravidin-biotinylated polyethylene glycol	10	$10 \sim 10^3$	3	29
fluorescence	fluorescein isothiocyannate labeled aptamer	5	5.64 ~ 100	3	30
fluorescence	Texas Red labeled peptide nucleic acid	10^4	-	2.5	31
fluorescence	FAM-cDNA	100	$1.28 \times 10^3 \sim 2.00 \times 10^7$	2	this study

Figure Captions

Figure 1. (a) TEM image, (b) UV-vis spectra, (c) Excitation spectrum (black line) and emission spectrum (red line) of GOQDs. Insets are digital photos of GOQDs under (1) visible and (2) UV light.

Figure 2. (a) Schematic illustration of the principle of fluorescent aptasensor for detection of *P. aeruginosa.* (b) Fluorescence emission spectra of FAM-cDNA, FAM-cDNA+GOQDs, FAM-cDNA+GOQDs+aptamer, and FAM-cDNA+GOQDs+aptamer+bacteria.

Figure 3. Optimization of the concentration of GOQDs. The fluorescence intensities were measured with the emission wavelength at 520 nm and excitation wavelength at 494 nm. Error bars indicate standard deviations (n = 3).

Figure 4. (a) Relationship of the fluorescence quenching process of FAM-cDNA by GOQDs with incubation time. (b) Relationship of the fluorescence restoration process of FAM-cDNA caused by target bacteria (10^7 cfu/mL) with incubation time. Experiment conditions: PBS buffer, 10 mM (pH 7.0); FAM-cDNA concentration, 50 nM; GOQDs concentration, 0.1 mg/mL; aptamer concentration, 50 nM. The fluorescence intensities were measured with the emission wavelength at 520 nm and excitation wavelength at 494 nm. Error bars indicate standard deviations (n = 3).

Figure 5. (a) Fluorescence emission spectra of FAM-cDNA@GOQDs@aptamer after incubation with different concentrations of *P. aeruginosa* (0, 1.28×10^3, 6.40×10^3, 3.20×10^4, 1.60×10^5, 8.00×10^5, 4.00×10^6, 2.00×10^7 cfu/mL). (b) Calibration plot of fluorescence intensity versus bacteria concentration. Experiment conditions: FAM-cDNA concentration, 50 nM; GOQDs concentration, 0.1 mg/mL; aptamer concentration, 50 nM. The fluorescence intensities were measured with the emission wavelength at 520 nm and excitation wavelength at 494 nm. Error bars indicate standard deviations (n = 3).

Figure 6. Specificity study of the fluorescent aptasensor towards *P. aeruginosa*. Experiment conditions: PBS buffer, 10 mM (pH 7.0); FAM-cDNA concentration, 50 nM; GOQDs concentration, 0.1 mg/mL; aptamer concentration, 50 nM. The fluorescence intensities were measured with the emission wavelength at 520 nm and excitation wavelength at 494 nm. The concentration of each bacterium is 10^5 cfu/mL. Error bars indicate standard deviations (n = 3).

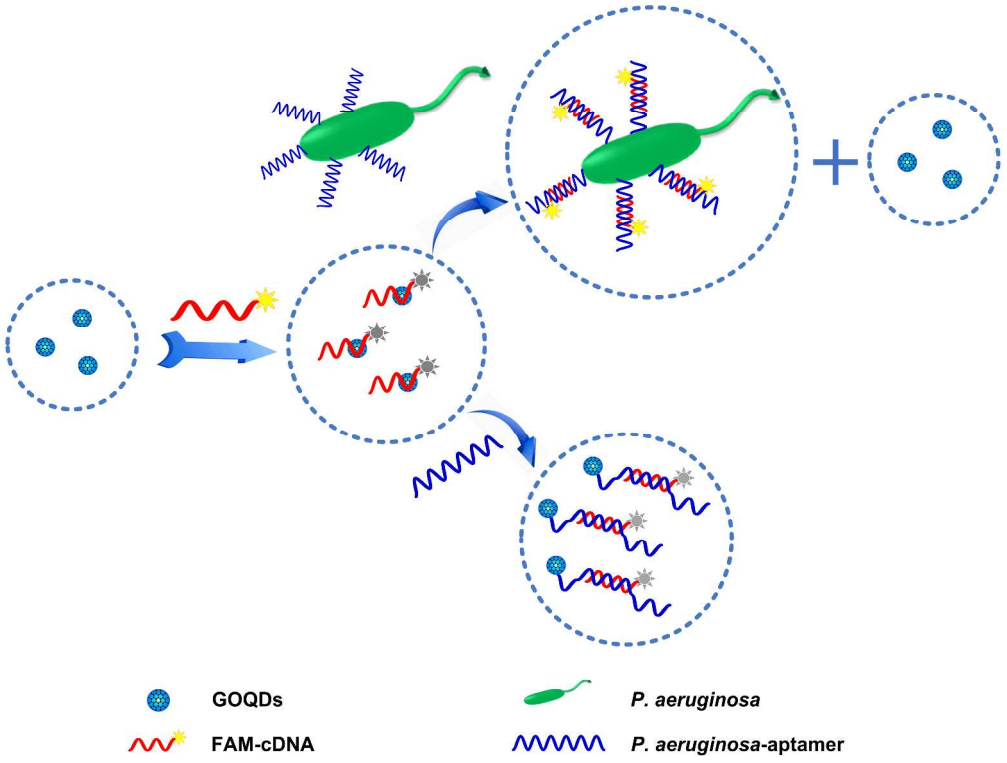

TOC

508x381mm (300 x 300 DPI)

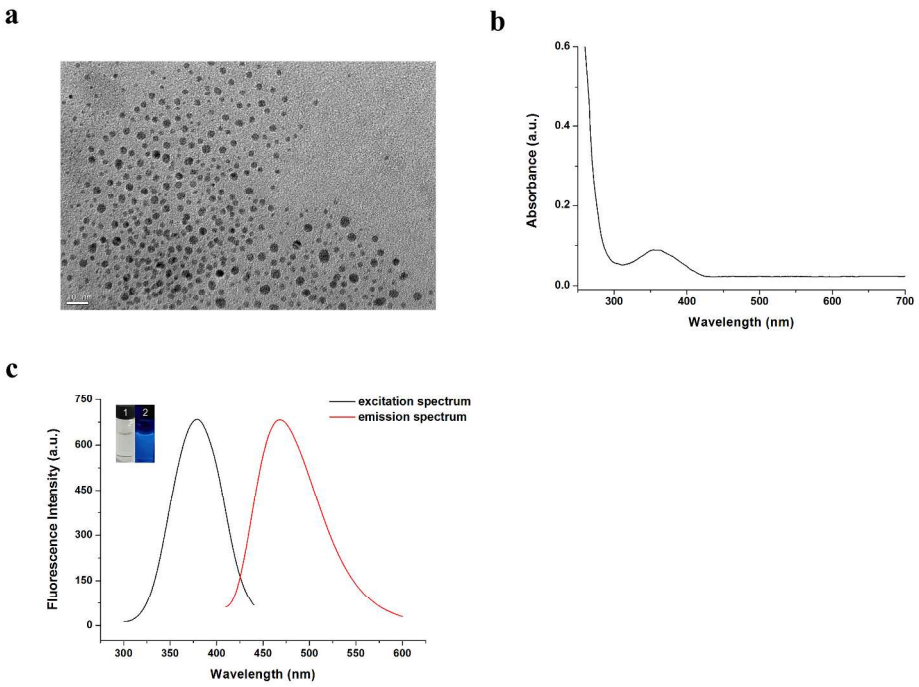

Figure 1

431x304mm (200 x 200 DPI)

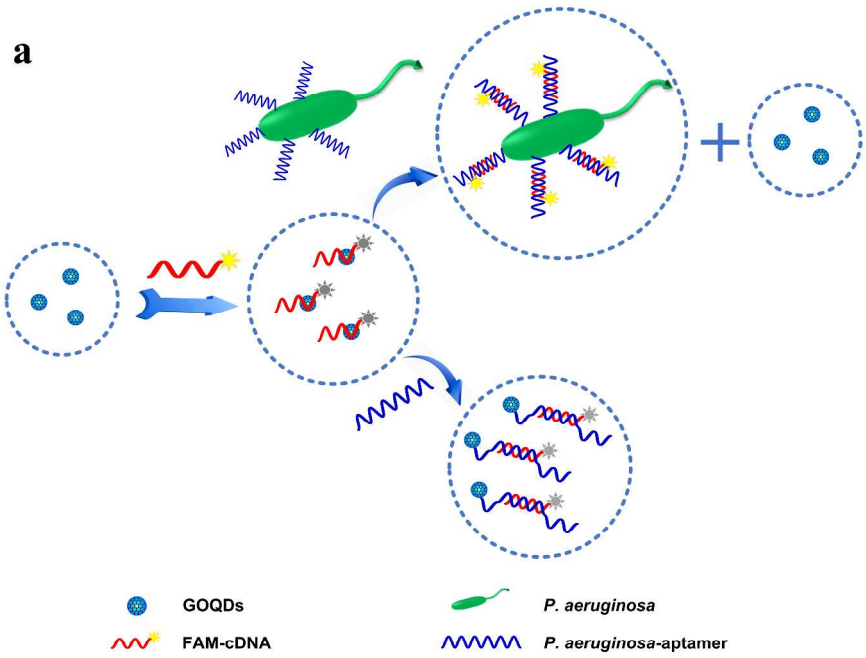

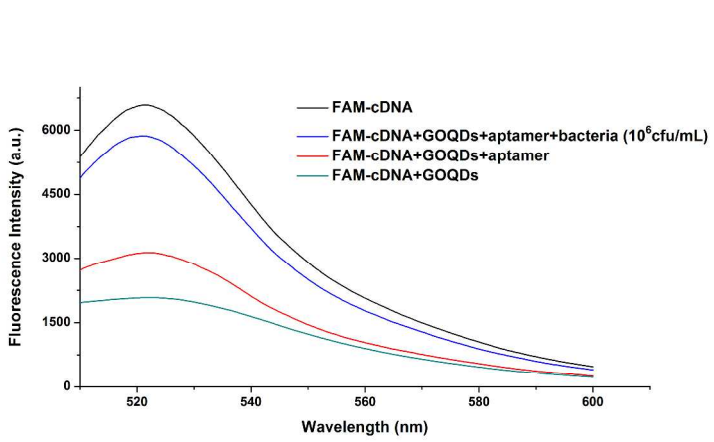

Figure 2

381x508mm (300 x 300 DPI)

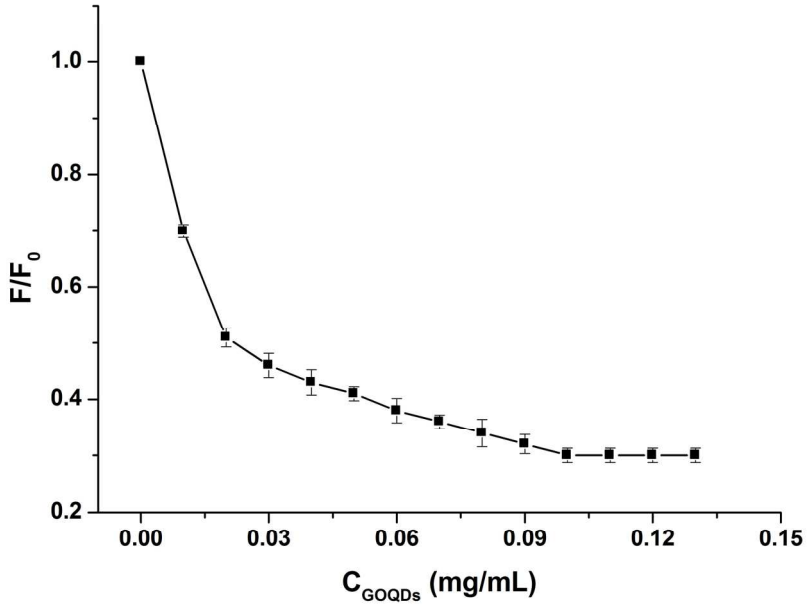

Figure 3

84x59mm (600 x 600 DPI)

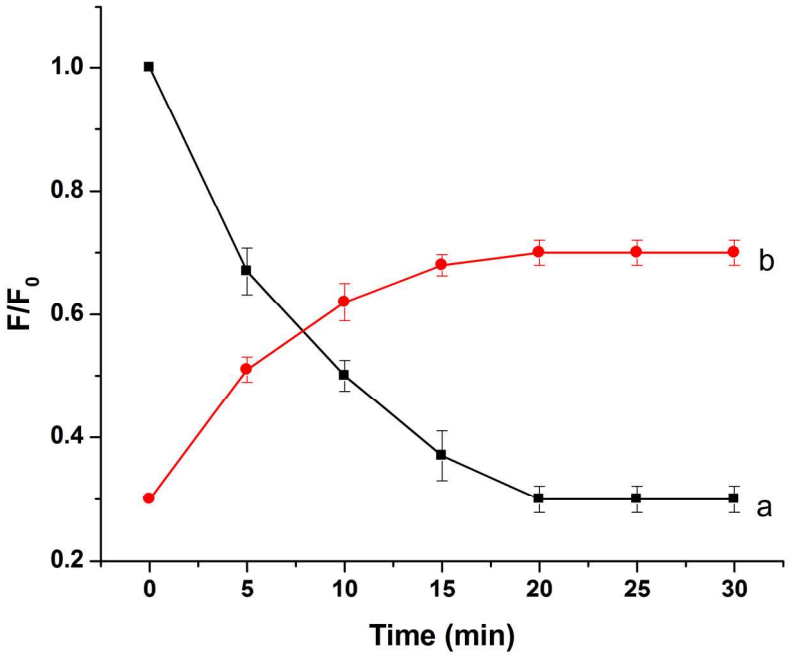

Figure 4

86x66mm (600 x 600 DPI)

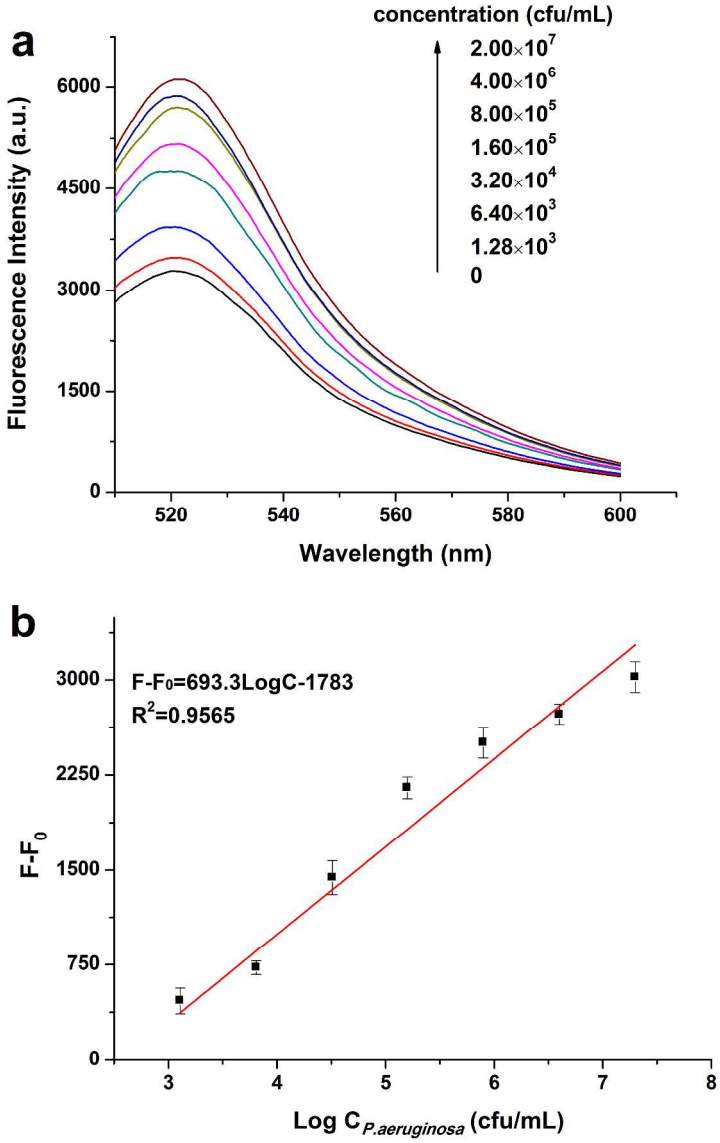

Figure 5

381x508mm (300 x 300 DPI)

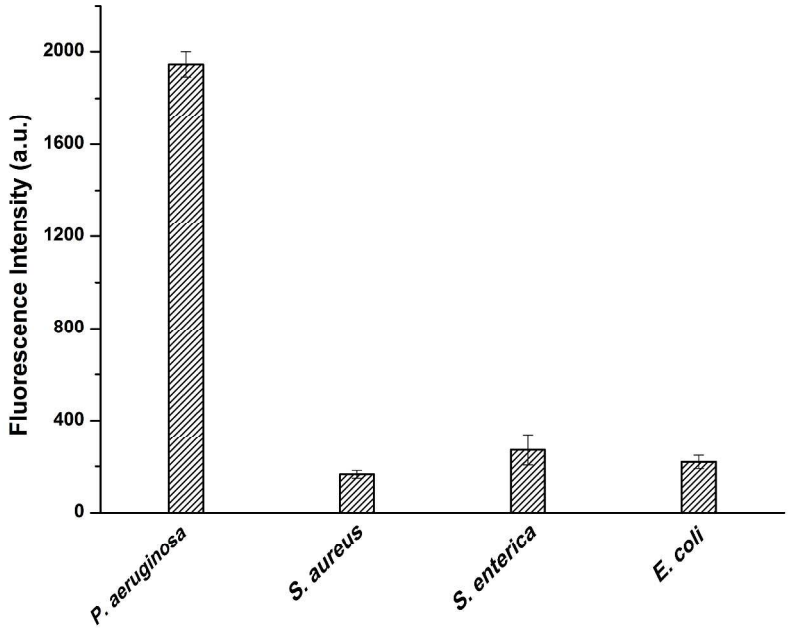

Figure 6

508x381mm (300 x 300 DPI)